

# Multi-Trait Genome-Wide Association Studies Reveal Loci Associated with Maize Inflorescence and Leaf Architecture

Brian R. Rice<sup>†</sup>, Samuel B. Fernandes<sup>†</sup> and Alexander E. Lipka<sup>\*</sup>

Department of Crop Sciences, University of Illinois, Urbana, IL, USA

<sup>\*</sup>Corresponding author: E-mail, alipka@illinois.edu.

<sup>†</sup>These authors contributed equally to this manuscript.

(Received January 24, 2020; Accepted March 17, 2020)

Maize inflorescence is a complex phenotype that involves the physical and developmental interplay of multiple traits. Given the evidence that genes could pleiotropically contribute to several of these traits, we used publicly available maize data to assess the ability of multivariate genome-wide association study (GWAS) approaches to identify pleiotropic quantitative trait loci (pQTL). Our analysis of 23 publicly available inflorescence and leaf-related traits in a diversity panel of  $n = 281$  maize lines genotyped with 376,336 markers revealed that the two multivariate GWAS approaches we tested were capable of identifying pQTL in genomic regions coinciding with similar associations found in previous studies. We then conducted a parallel simulation study on the same individuals, where it was shown that multivariate GWAS approaches yielded a higher true-positive quantitative trait nucleotide (QTN) detection rate than comparable univariate approaches for all evaluated simulation settings except for when the correlated simulated traits had a heritability of 0.9. We therefore conclude that the implementation of state-of-the-art multivariate GWAS approaches is a useful tool for dissecting pleiotropy and their more widespread implementation could facilitate the discovery of genes and other biological mechanisms underlying maize inflorescence.

**Keywords:** GWAS • Inflorescence • Maize • Multivariate • Pleiotropy • Simulations.

## Introduction

Complex biological phenotypes in plants result from the input and interactions of multiple phenotypic traits. Inflorescence in maize (*Zea mays* L.), for instance, reflects the interplay between tassel, ear and vegetative traits (Bonnett 1954). To be successful, modern maize breeding requires optimal inflorescence, specifically the temporal syncing of pollen shedding and receptive silks. Such a relationship is highly adapted to local environmental conditions and dependent upon the vegetative structure of the plant (Bouchet et al. 2013). In conjunction with this, modern agriculture is pushing for unprecedented levels of planting density (Shi et al. 2016) and a more upright leaf angle will allow for better circulation in an open pollination field. To date, several quantitative trait loci (QTL) have been identified that

contribute to optimal maize inflorescence and plant leaf architecture (Buckler et al. 2009, Brown et al. 2011, Tian et al. 2011, Li et al. 2015, Calderón et al. 2016, Wu et al. 2016, Pan et al. 2017). Some genetic components underlying these QTL might contribute to two or more of these traits, a phenomenon called pleiotropy (Stearns 2010). This theory is supported by QTL regions identified for both tassel (Brown et al. 2011, Wu et al. 2016) and leaf traits (Tian et al. 2011) near the *liguleless* (*lg*) genes. *Liguleless1* (*lg1*) particularly has strong evidence for a pleiotropic relationship to maize leaf and inflorescence traits (Foster et al. 2004, Lewis et al. 2014). This and other *lg* gene mutants (i.e. *lg2*, 3 and 4) alter leaf angle by removing the ligule while simultaneously affecting tassel branch initiation. In addition, genes expressed at the initiating ligules are co-expressed in tassel branches (Johnston et al. 2014). It is because of this evidence, and their relationship for successful pollination and seed set, that more pleiotropic QTL (pQTL) for maize inflorescence and leaf traits are hypothesized to exist.

One common practice for addressing pleiotropy is to compare results across univariate studies, where results from multiple single-trait genome-wide association studies (GWASs) are combined to identify statistically significant marker–trait associations (Wei and Johnson 1985). The procedure consists of performing a separate GWAS for each trait. Ideally, pQTL would then manifest themselves as one of the peak marker–trait associations across multiple single-trait GWASs (Visscher and Yang 2016, Chai et al. 2018). Alternatively, post hoc procedures could be implemented to compile univariate GWAS information (i.e. effect estimates, *P*-values) for each marker and then make pleiotropic inferences (Huang et al. 2011, O'Reilly et al. 2012, Sluis et al. 2013).

When multiple traits are collected on the same individuals within a study, more formal multivariate statistical methods are available to detect pQTL and are generally categorized into two different approaches (Solovieff 2013, Galesloot et al. 2014). The first uses a mixed linear model (MLM) with a matrix of correlated traits as the response variable. Such multivariate MLMs (mvMLMs) are commonly applied in plants (Carlson et al. 2019), where it includes covariates to reduce false positives that arise from population structure and kinship (Zhou and Stephens 2014). The second approach utilizes data reduction methods to create composite traits (Klei et al. 2008). One such method converts  $t$  traits into  $t$  linearly uncorrelated principal components (PCs; Hotelling 1933). Each of these PCs can then

be used in univariate GWAS to identify genomic regions with peak-associated markers. Genomic marker data associated with these PCs are hypothesized to be jointly linked to the traits of interest (Zhang *et al.* 2018). All PCs, including those explaining even a small amount of variation, could be useful for identifying pQTL (Avery *et al.* 2011, Liu *et al.* 2012, Aschard *et al.* 2014). Any detected pQTL can then rely on the loadings, which explain each trait's contribution to the total variation in a given PC, for biological interpretation.

To ensure that the biology underlying inflorescence is understood and utilized as effectively as possible in maize breeding, the advantages and disadvantages of these pQTL approaches need to be rigorously assessed using maize data. Therefore, we performed univariate, multivariate, and PC-based GWASs using publicly available maize leaf and inflorescence data. In addition, we used maize genotypic data to conduct a simulation study to compare the true- and false-positive detection rates of simulated quantitative trait nucleotides (QTNs) using these approaches. We hypothesized that the resulting peak-associated single-nucleotide polymorphisms (SNPs) using real data are linked to loci that simultaneously contribute to the variability of maize leaf and inflorescence traits.

## Results

A total of 23 traits related to maize inflorescence organs and leaf architecture were analyzed. The genetic correlation between 21 nonflowering time traits closely resembled the phenotypic correlation (Fig. 1). The multivariate analysis of these publicly available maize traits detected multiple peak-associated SNPs that were consistent with those identified in the previous studies (Table 1). In addition, the simulation study revealed that multivariate approaches yielded higher true-positive detection rates relative to univariate approaches, particularly in cases where the

simulated trait heritabilities were medium and/or low. The entire list of marker *P*-values for all publicly available trait analyses can be accessed at <https://github.com/lipka-lab/Multi-Trait-GWAS-Methods-Reveal-Loci-Associated-with-Maize-Inflorescence-and-Leaf-Architecture>.

### Univariate GWAS

To aid in distinguishing between trait-specific and pleiotropic genomic signals, univariate GWAS was performed on each trait independently (Table 1). These univariate analyses identified significant peak associations present on chromosomes 1, 2, 3 and 8 for growing degree days (GDD) to silk and GDD to tassel resemble similar published associations for flowering time (Buckler *et al.* 2009, Peiffer *et al.* 2014). Two SNPs on chromosome 2 were declared significant for both tassel primary branches [TPBs; at 1% false discovery rate (FDR)] and main spikelet length (MSL; at 5% FDR). These SNPs were within 2 Mb from a QTL region found by Wu *et al.* (2016) for tassel branch number (TBN) and tassel length (TL). Finally, an SNP on chromosome 9 was declared significant at 10% FDR for ear diameter (ED). No associations for any maize ear-related traits have been previously identified in the surrounding region; however, this SNP was 66 kb from a QTN found to be significant for TL by Wu *et al.* (2016). For all these SNPs, it is expected that the distance to previously published peaks may change depending on which version of the maize reference genome the authors used. Nevertheless, the univariate results demonstrated that our methods can replicate similar findings of more statistically powerful univariate studies.

### Multivariate GWAS

Multivariate mixed-model GWAS was performed on TPB, upper leaf angle (ULA) and ear row number (ERN). Both GDD to silk and tassel were still included as covariates to prevent spurious associations due to flowering time. Interestingly, the model with

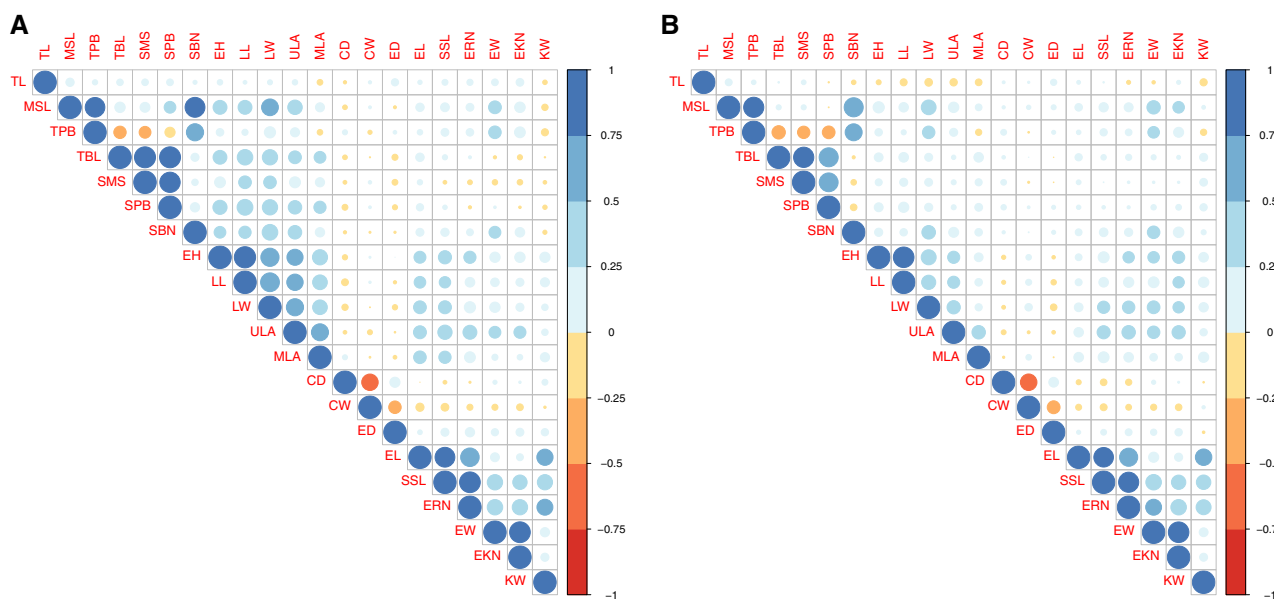


Fig. 1 Trait correlations. (A) Pearson correlations of the BLUPs of 21 inflorescence and leaf-related traits. (B) Pearson correlations of the estimated additive marker effects from the univariate GWAS conducted on each of these 21 traits.

**Table 1** List of peak-associated single-nucleotide polymorphisms

Chromosome	AGPv4 position	Analysis <sup>a</sup>	P-values <sup>b</sup>	MAF
1	20,835,743	PC11	$2.39 \times 10^{-6}$	0.2046
1	277,120,730	GDD to silk	$2.63 \times 10^{-6}$	0.0961
2	18,185,025	GDD to silk	$2.65 \times 10^{-6}$	0.0996
2	179,171,874	PC5	$8.90 \times 10^{-7}$	0.1428
2	29,749,088	PC5	$3.04 \times 10^{-7}$	0.4517
3	161,013,215	GDD to silk	$4.88 \times 10^{-7}$	0.3736
3	161,013,240	GDD to silk	$1.22 \times 10^{-6}$	0.3772
3	161,013,249	GDD to silk	$4.88 \times 10^{-7}$	0.3736
3	161,013,251	GDD to silk	$1.22 \times 10^{-6}$	0.3772
3	161,168,101	GDD to silk	$1.02 \times 10^{-6}$	0.2669
3	200,352,075	TPB, MSL, MV	$4.05 \times 10^{-8}$ , $2.30 \times 10^{-7}$ , $6.52 \times 10^{-7}$	0.3381
3	200,352,109	TPB, MSL, MV	$4.05 \times 10^{-8}$ , $2.30 \times 10^{-7}$ , $6.52 \times 10^{-7}$	0.3381
6	142,569,704	MV	$6.46 \times 10^{-8}$	0.068
8	134,706,486	GDD to silk	$1.80 \times 10^{-6}$	0.1619
8	1,351,014,06	GDD to tassel, GDD to silk	$4.87 \times 10^{-9}$ , $1.27 \times 10^{-9}$	0.2028
9	103,121,862	ED	$2.26 \times 10^{-7}$	0.0818

<sup>a</sup>Refer to **Supplementary Table S1** for abbreviations of trait names.

<sup>b</sup>For single-nucleotide polymorphisms significant in more than one analysis, unadjusted P-values are listed in the same order as their respective analysis.

the optimal BIC was one that included no fixed-effect covariates controlling for population structure.

One SNP was statistically significantly associated with these traits at 5% FDR, and an additional two SNPs were statistically significant at 10% FDR (**Fig. 2**). The most significant of these is located in a region on chromosome 6 similar to QTLs reported for TL by Wu et al. (2016) and Brown et al. (2011). The others are located 34 bp apart from one another on chromosome 3 and were also significantly associated with TPB and MSL in the univariate GWAS (**Table 1**). These SNPs were the only results found significant in more than one of the tested GWAS approaches. Because the alternative hypothesis for the multivariate model states that at least two traits have a nonzero additive association with a genomic marker, these results provide evidence that these traits are associated with at least two of the traits.

## PC GWAS

PC GWAS using the unified MLM was conducted for 18 of a possible 21 PCs of maize ear-, tassel- and leaf-related traits. There were no reasonable overlaps between significant SNPs in PC GWAS and mvGWAS. Overall, a single SNP on chromosome 2 was declared significant (at 10% FDR) for PC5 (**Fig. 3**). The variability in PC5 is mainly contributed to the variation in tassel, ear and leaf traits (**Fig. 3B**). Interestingly, this SNP was within 0.695 and 0.17 Mb of two SNPs found significant for TL and TBN (Wu et al. 2016), respectively. No other SNPs for PC GWAS were declared significant at 5% or 10% of FDR; however, if the FDR threshold was relaxed to 20%, associations on chromosome 1 and chromosome 8 were identified for PC11 (**Fig. 4**). Visual evaluation for PC11 shows that these marker P-values diverge from the expected distribution of P-values under the null hypothesis of no marker–trait association (**Fig. 4A**).

Evaluation of the loadings of PC11 revealed that secondary branch number and kernel weight made the strongest positive contributions to PC11, while cob weight and cob diameter made the strongest negative contributions (**Fig. 4B**). These results give credence for follow-up studies to investigate these signals.

## Simulation study

To evaluate the false-positive rate of these methods, a set of three simulated traits with a narrow-sense heritability of  $h^2 = 0$  and no underlying QTNs were replicated 1,000 times (**Fig. 5**). As expected, the Bonferroni threshold had a lower false-positive rate than an FDR approach, as it is commonly known to be excessively conservative at a high number of tests (Frane 2015). Multivariate mixed-model GWAS had the highest proportion of false positives. Nonetheless, the observed false-positive rates are at or below the theoretical values, suggesting that all approaches adequately adjusted for false positives.

Multivariate mixed-model GWAS and GWAS on PC1 (abbreviated PC1 GWAS) consistently had the highest true-positive rate across all settings (**Fig. 6**). However, when all heritabilities were 0.9, GWAS on the individual traits detected pleiotropic QTN as well as multivariate approaches. In contrast, for medium- or low-trait heritabilities (0.5 and 0.2, respectively), the multivariate methods consistently had higher true-positive rates than univariate analyses. Across the multi-trait methods, mvGWAS had a slightly higher true-positive detection rate than the PC1 GWAS when all of the simulated trait heritabilities were either 0.9 or 0.5. In the settings where the heritabilities simulated were identical across all traits, the true-positive detection rate of PC3 GWAS was lowest among the multivariate approaches. In contrast, when a mixture of heritabilities was simulated (e.g. 0.2, 0.5 and 0.9), PC3 GWAS tended to yield a

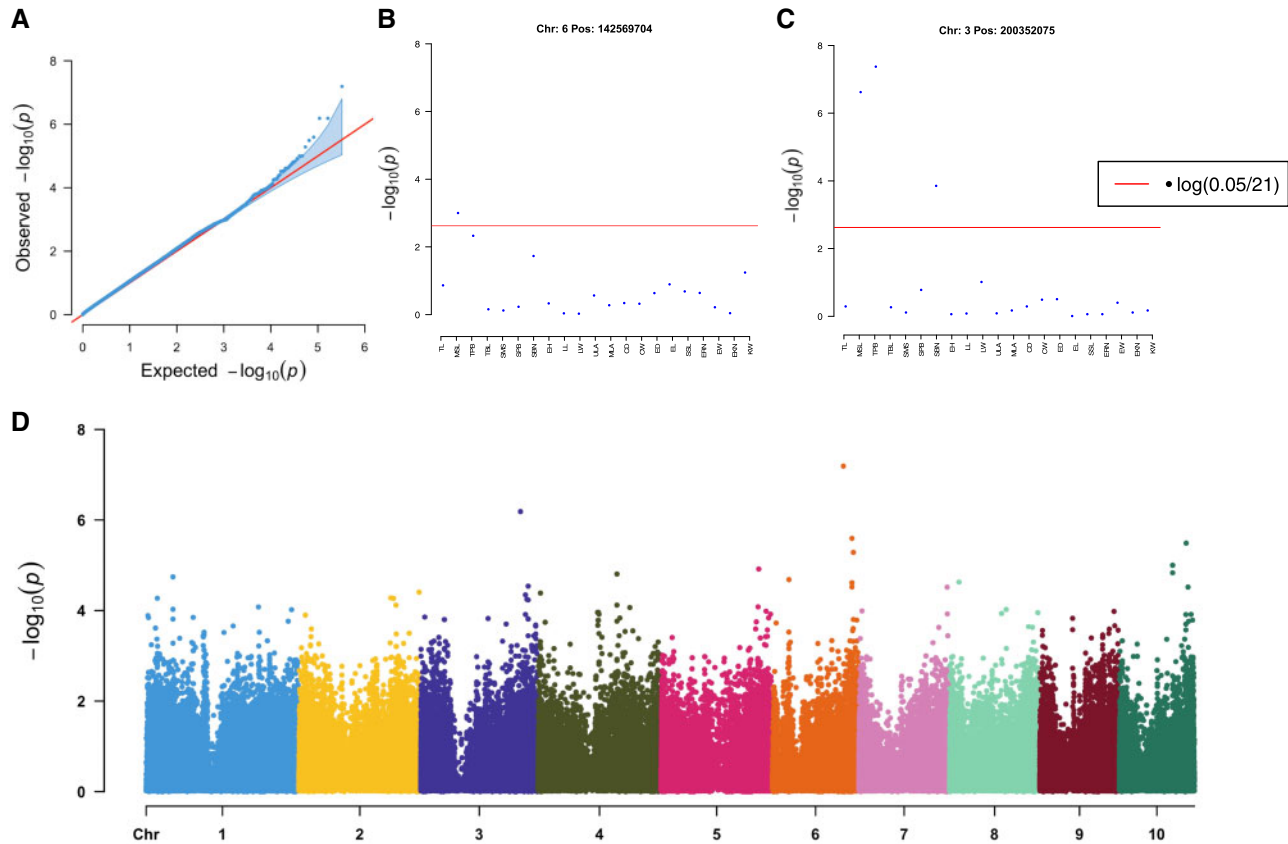


**Fig. 2** Multivariate genome-wide association results for TPBs, ULA and ERN. (A) Distribution of observed vs. expected  $-\log_{10} P$ -values from the multivariate GWAS conducted on TPB, ULA and ERN. (B)  $-\log_{10} P$ -values (y-axis) for a peak-associated marker (located on chromosome 6, base pair position 142,569,704) obtained for each of the univariate GWAS conducted individually on the 21 studied traits (x-axis). (C)  $-\log_{10} P$ -values (y-axis) for a peak-associated marker (located on chromosome 3, base pair position 200,352,075) obtained for each of the univariate GWAS conducted individually on the 21 studied traits (x-axis). (D) Manhattan plot where the  $-\log_{10} P$ -values (y-axis) from the multivariate GWAS conducted on TBN, ULA and ERN. All marker coordinates correspond to B73 RefGen\_v4.

higher true-positive detection rate than PC1 or PC2 GWAS. Finally, similar results were obtained whether or not the simulated traits consisted of purely of pleiotropic QTNs. However, the traits with only pleiotropic QTNs had higher observed true-positive detection rates than their equivalent settings that included both pleiotropic and non-pleiotropic QTNs.

## Discussion

We used simulated and publicly available maize traits related to inflorescence to test the ability of several univariate and multivariate GWAS approaches to identify pQTL. Our results suggest that each of these approaches was capable of identifying such signals, albeit with varying levels of success. That is, each of the univariate and multivariate GWAS approaches identified genomic signals for inflorescence-related traits that were consistent with those found in previous studies. The simulation studies demonstrated the advantage of multivariate approaches when traits with low-to-moderate heritabilities or traits with a mixture of low-to-high heritabilities were analyzed in one multivariate model. Collectively, our analyses of real and simulated traits demonstrate that these tested GWAS approaches can facilitate the elucidation of genomic regions likely to contain

causal mutations underlying multiple traits and this could substantially assist follow-up biological studies dedicated to dissecting pleiotropy.

## Advantages and disadvantages of each approach

The identification of pleiotropy is important because marker-assisted selection on favorable alleles of pleiotropic loci could lead to a simultaneous change in multiple agronomically important traits (Chai *et al.* 2018). Although the analyses explored in this work are statistical approaches and therefore not capable of illuminating the biological function of putatively pleiotropic causal mutations, we nevertheless illustrated their usefulness. Moreover, each of the analyses we considered had advantages that contributed unique insight into the characterization of pleiotropy. For example, the univariate GWAS approaches were capable of identifying associations for traits that were previously identified for other traits [e.g. a signal we identified for ED was physically close to an association for TL reported in Wu *et al.* (2016)]. Similarly, the PC GWAS approach also identified signals that collectively contributed to tassel, ear and leaf traits. Finally, multivariate GWAS complemented univariate PC GWAS by identifying an additional signal on chromosome 6 associated with TPB, ULA and ERN. Thus, our recommendation

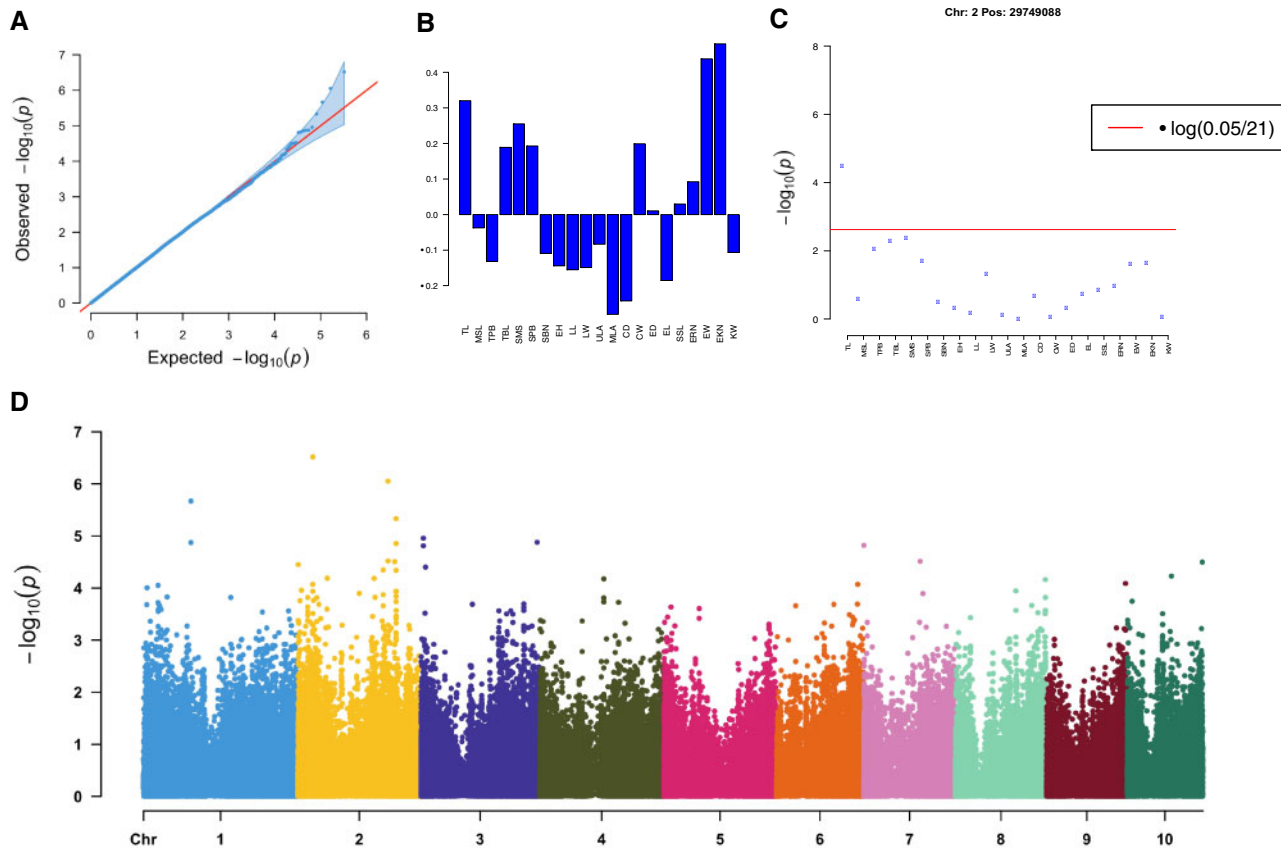


**Fig. 3** Genome-wide association results for PC5. (A) Distribution of observed vs. expected  $-\log_{10} P$ -values from the GWAS conducted on PC5. (B) Observed loadings from PC5 ( $y$ -axis) for each trait ( $x$ -axis). (C)  $-\log_{10} P$ -values ( $y$ -axis) for the peak marker associated with PC5 (located on chromosome 2, base pair position 29,749,088) for each univariate GWAS conducted on the traits contributing to PC5 ( $x$ -axis). (D) Manhattan plot where the  $-\log_{10} P$ -values ( $y$ -axis) from the GWAS conducted on PC5 are plotted for each marker according to its base pair and chromosome position. All marker coordinates correspond to B73 RefGen\_v4.

for future association studies is to use all of these GWAS approaches so that as complete a picture of the pleiotropic landscape as possible can be ascertained.

Despite the potential for biological insight into putative pQTL provided by the approaches we explored, each of these GWAS approaches had their drawbacks. By design, univariate GWAS is technically not a multivariate method and thus can only account for the variation in multiple traits if they are included as covariates in the GWAS model. Even though PC GWAS can easily accommodate a large number of traits, the biological interpretation of each PC might be difficult. Moreover, if a genomic signal was to be identified as associated with a PC, there is some ambiguity as to whether the association holds for one or more of the traits contributing the most to that PC (i.e. the traits with the largest absolute values of the loadings) and to any insight this identified signal can provide for the genetic architecture of these traits.

The most practical drawback of the multivariate GWAS approach is that it becomes extremely computationally intensive when a large number of traits are analyzed (Zhou and Stephens 2014). Based on the findings from our study, we agree with Zhou and Stephens (2014) that analyzing a maximum of three to five traits ensures that the computational time required does not become cumbersome. Our multivariate GWAS took approximately

12 min to complete on a 64-GB RAM machine. On this same machine, an attempt to analyze 10 traits was aborted after it was estimated to take 6 weeks to complete. In contrast, a PC GWAS that included all available traits required the same computational resources as equivalent univariate GWAS. Another drawback with multivariate GWAS is similar to one noted for PC GWAS in that the identification of a multivariate genomic signal will not necessarily mean that all of the evaluated traits have causal mutations in the genomic region surrounding the identified pQTL. Lastly, we tentatively recommend using the leave one chromosome out (LOCO) approach for multivariate GWAS (Fatumo et al. 2019), as we expect the same advantages noted for using LOCO in univariate GWAS [reported in Rincant et al. (2014), Chen and Lipka (2016)] to be observed. Before we can recommend this LOCO approach in plants without hesitation, we suggest that follow-up studies thoroughly compare LOCO multivariate GWAS to non-LOCO multivariate GWAS.

### Simulation study suggests that multivariate approaches outperform univariate approaches in maize

Our simulation compared the ability of two multi-trait GWAS approaches to detect pleiotropic QTN but was not exhaustive.

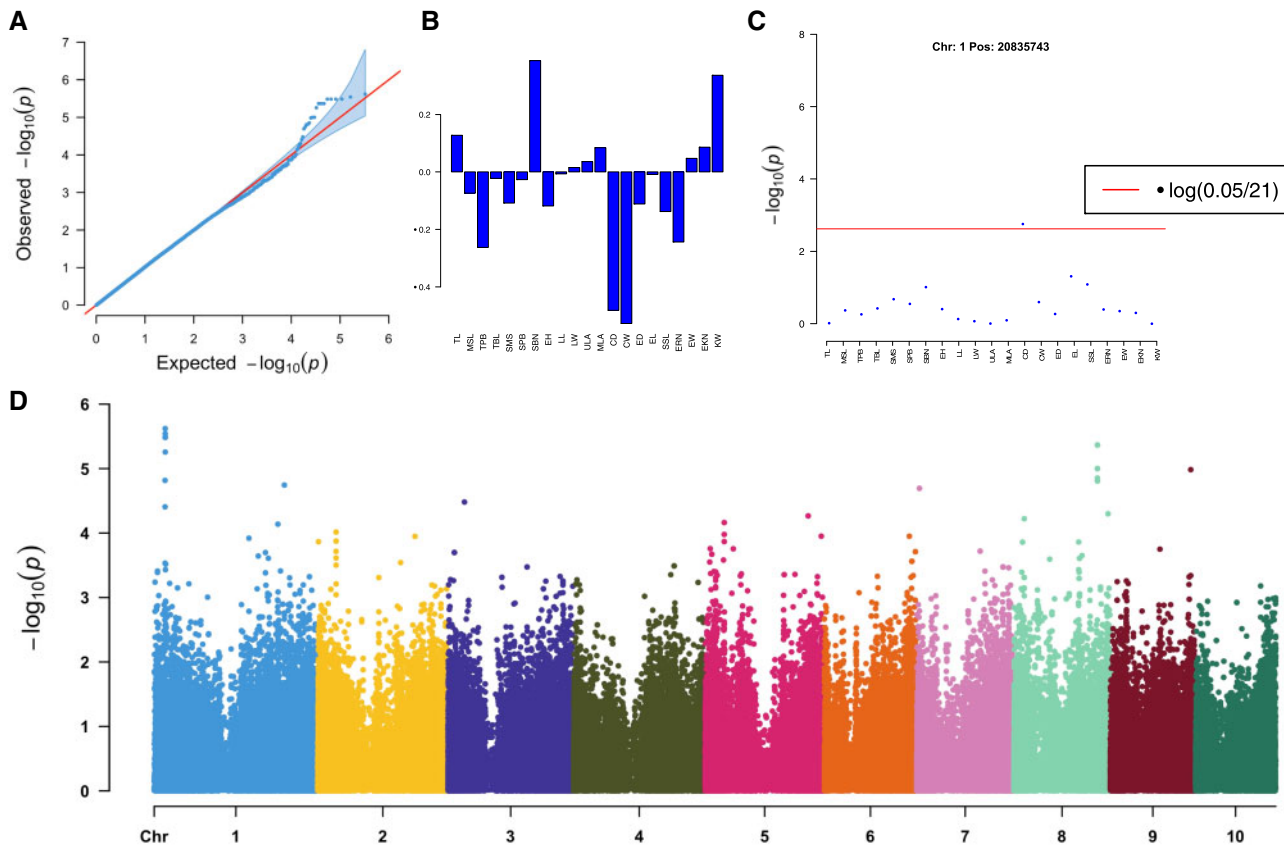


**Fig. 4** Genome-wide association results for PC11. (A) Distribution of observed vs. expected  $-\log_{10} P$ -values from the GWAS conducted on PC11. (B) Observed loadings from PC11 (y-axis) for each trait (x-axis). (C)  $-\log_{10} P$ -values (y-axis) for the peak marker associated with PC11 (located on chromosome 1, base pair position 20,835,743) for each univariate GWAS conducted on the traits contributing to PC11 (x-axis). (D) Manhattan plot where the  $-\log_{10} P$ -values (y-axis) from the GWAS conducted on PC11 are plotted for each marker according to its base pair and chromosome position. All marker coordinates correspond to B73 RefGen\_v4.

The simulation was limited in scope to the population structure and linkage disequilibrium (LD) decay present in this specific maize diversity panel. Under these constraints, there was no indication that mvMLM or PC GWAS had inflated false-positive rates. When considering the range of situations tested, both approaches had comparable true-positive rates. However, as expected due to added variation, the true-positive rate decreased when non-pleiotropic QTNs were introduced. Of particular interest was the finding that multivariate models appeared to have an advantage over univariate ones when a range of high- to low-heritable traits was analyzed. This is supported by similar findings from multi-trait genomic selection studies (Jia and Jannink 2012, Fernandes *et al.* 2018).

Settings were chosen to blueprint simple cases of pleiotropic traits where only a few casual mutations controlled the majority of variation. Narrow-sense heritabilities for simulated traits followed the same range of those of the real traits (Table 2 and Supplementary Table S1). The narrow-sense heritabilities of traits chosen for mvMLM (i.e. TPB, ULA and ERN; Supplementary Table S1) resembled setting 5 the closest in that they were all low (i.e.  $\sim 0.2$ ). Follow-up studies should look at a wider range of genetic architectures, including more complex traits with a mixture

of additive and nonadditive pleiotropic QTNs, and measures should be taken to directly control the correlation between the simulated traits. Moreover, given that simplePHENOTYPES allows for either control of trait heritabilities (and QTN effect sizes) or trait correlations, and not both, we opted to control the trait heritabilities directly because it gave us more control over the traits we simulated. It is important to point this limitation out because the correlations of our simulated traits were all much higher than the correlation of our real traits in most cases.

Finally, the simulation studies provided some potential insight into the findings from the analysis of 23 maize inflorescence-related traits. That is, the discrepancies in results between methods for the real trait analysis were likely not due to false associations but possibly from other factors including the underlying genetic complexity of the traits and the underlying cause of the pleiotropic signal detected by each method (see Stearns 2010, Solovieff 2013, Gianola *et al.* 2020 for review of mechanisms underlying pQTL). Further exploration into pQTL identified in the analysis of the real traits reported here will shed light on the degree to which the multivariate GWAS approaches here can distinguish between biological mechanisms underlying putative pleiotropic signals.

## Conclusion

The identification of pQTL associated with maize inflorescence and related vegetative traits is important because it could result

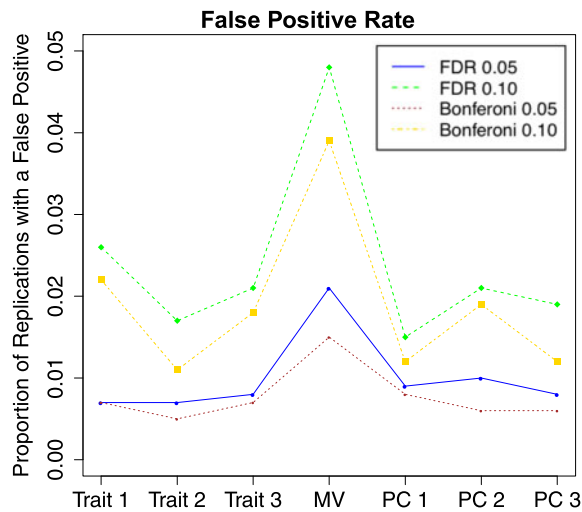


**Fig. 5** False-positive rates for the simulation study. The false-positive rate is reported as the proportion of 1,000 replicate traits from the simulation setting with no underlying QTN where at least one statistically significant SNP association was identified. These proportions are presented on the *y*-axis. The *x*-axis displays the GWAS model being used, particularly univariate GWAS (traits 1–3), multivariate GWAS (MV) and PC GWAS (PCs 1–3). Results are reported for a Bonferroni control of the experiment-wise (i.e. genome-wide) type I error rate of  $\alpha = 0.05$  and  $\alpha = 0.10$ , as well for the Benjamini–Hochberg procedure to control the FDR at 0.05 and 0.10.

in the simultaneous genetic gain of maize inflorescence as a whole instead of on only an individual trait. The work presented in this study facilitates such an endeavor by showing that it is practical to use currently available multivariate GWAS approaches in a concerted manner to find pQTL and hence facilitate the identification of pleiotropic causal mutations. We recommend that future research into multivariate GWAS software development focuses on implementing approaches that can dissect which subsets of traits have pQTL in a computationally efficient manner; particularly noted that a pitfall of current multivariate approaches is that it is difficult to elucidate which traits have nonzero effects at a given pQTL. Nevertheless, we clearly show that the tested multivariate approaches have their greatest advantages over univariate approaches when correlated traits with low, medium and high heritabilities are considered in one analysis. Thus, we conclude that one of the greatest advantages of pQTL analyses is its potential to facilitate the quantification of the genetic architecture of low-heritable traits that are correlated with higher-heritable traits.

## Materials and Methods

### Phenotypic and genotypic data

We analyzed a total of 23 publicly available inflorescence and leaf-related traits in the 281-member Goodman–Buckler diversity panel (Flint-Garcia et al. 2005) measured in up to 10 environments (Supplementary Table S1) (for information on experimental design and data collection for this public data set, see Buckler et al. 2009, Brown et al. 2011, Tian et al. 2011, Peiffer et al. 2014). Best linear unbiased predictors (BLUPs) for each phenotype were predicted from a generalized mixed model fitted across these environments using GLMER in R

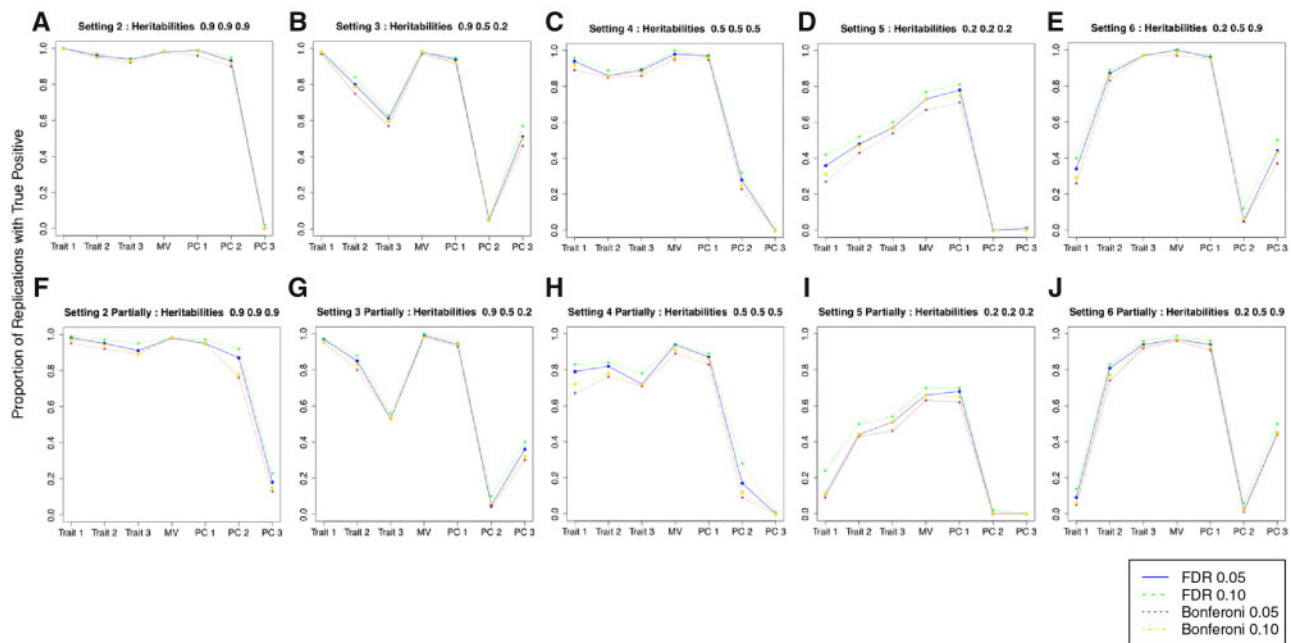


**Fig. 6** True-positive rates for the simulation study. For each simulation setting (A–J), the true-positive rate is reported as the proportion of 100 replicate traits with at least one statistically significant SNP association within  $\pm 250$  kb of a quantitative trait nucleotide. These proportions are presented on the *y*-axis. The *x*-axis displays the GWAS model being used, particularly univariate GWAS (traits 1–3), multivariate GWAS (MV) and PC GWAS (PCs 1–3). Results are reported for a Bonferroni control of the experiment-wise (i.e. genome-wide) type I error rate of  $\alpha = 0.05$  and  $\alpha = 0.10$ , as well for the Benjamini–Hochberg procedure to control the FDR at 0.05 and 0.10.

**Table 2** Simulation parameters

Simulation setting	Trait $h^2$	Number of pleiotropic QTNs	Largest QTN effect size (traits: 1–3) <sup>a</sup>	Number of trait-specific QTNs	Realized correlation with traits 1 and 2	Realized correlation with traits 1 and 3	Realized correlation with traits 2 and 3
Setting 1 null trait	0, 0, 0	0	0, 0, 0	0	0	0	0
Setting 2	0.9, 0.9, 0.9	3	0.9, 0.5, 0.2	0	0.9219	0.7607	0.9470
Setting 2 partially	0.9, 0.9, 0.9	3	0.9, 0.5, 0.2	2	0.7693	0.6310	0.9353
Setting 3	0.9, 0.5, 0.2	3	0.9, 0.5, 0.2	0	0.9222	0.7678	0.9512
Setting 3 partially	0.9, 0.5, 0.2	3	0.9, 0.5, 0.2	2	0.7719	0.6331	0.9378
Setting 4	0.5, 0.5, 0.5	3	0.9, 0.5, 0.2	0	0.9201	0.7579	0.9478
Setting 4 partially	0.5, 0.5, 0.5	3	0.9, 0.5, 0.2	2	0.7718	0.6376	0.9380
Setting 5	0.2, 0.2, 0.2	3	0.9, 0.5, 0.2	0	0.9201	0.7579	0.9478
Setting 5 partially	0.2, 0.2, 0.2	3	0.9, 0.5, 0.2	2	0.7649	0.6398	0.9372
Setting 6	0.2, 0.5, 0.9	3	0.9, 0.5, 0.2	0	0.9186	0.7465	0.9433
Setting 6 partially	0.2, 0.5, 0.9	3	0.9, 0.5, 0.2	2	0.7644	0.6279	0.9375

For each simulation setting, the narrow-sense heritabilities and other parameters of traits 1–3 are given. For each setting, an identical setting (i.e. 'partially') that included additional trait-specific QTNs was simulated. The number of simulated trait-specific QTNs is reported. The remainder of simulation settings was constant across simulations settings. The average Pearson correlation between each trait combination across replicates is given.  $h^2$ , narrow-sense heritability.

<sup>a</sup>For a given trait, the largest QTN effect sizes ( $\alpha$ ) are chosen and the remainder follows a geometric series where the  $i$ th QTN has the effect size of  $\alpha^i$ . The  $j$ th trait-specific QTN has an effect size that continues the geometric series (i.e.  $\alpha^{3+j}$ ).

(Bates et al. 2015, R Core Team 2019). For traits that were approximately normally distributed, the following model was used:

$$Y_{ij} = \mu + G_i + \text{Env}_j + \epsilon_{ij}, \quad (1)$$

where the response variable ( $Y_{ij}$ ) is the observed phenotypic value of the  $i$ th genotype grown in the  $j$ th environment,  $\mu$  is the grand mean,  $G_i$  is the random effect of the  $i$ th genotype,  $\text{Env}_j$  is the random effect of the  $j$ th environment and  $\epsilon_{ij}$  is the error term for the  $i$ th genotype grown in the  $j$ th environment. For traits that followed a gamma distribution (positively skewed), a similar generalized linear model (GLM) with the negative inverse link function was used. For traits that were collected as count data (i.e. positive integers, assumed to follow a Poisson distribution), a similar GLM with the natural logarithm link was used. If the model fitting procedure for these GLMs failed to converge and a normal distribution could be reasonably assumed, then the identity link function was used; otherwise, traits were transformed using a quartile transformation (Gilchrist 2000) performed with the *qnorm* R function (van den Boogaart and Tolosana-Delgado 2008). The resulting transformed data were assumed to follow a normal distribution. For phenotypes where the effect size of environment was close to zero, the  $\text{Env}_j$  term was dropped from the model to avoid a singular fit. To improve the accuracy of BLUPs, an additional 5,702 recombinant inbred lines from the nested association mapping panel (Yu et al. 2008, McMullen et al. 2009) were used in model (1). Due to the nested structure of this panel, these additional 5,702 lines were not included in further analyses. For each trait, the BLUPs of the genotype effects were used as the response variables for GWAS.

A mixed model where the response variable was either a PC or trait BLUP and the explanatory variable was the individual genotype effect with a covariance matrix corresponding to the VanRaden additive effect matrix was used to estimate narrow-sense heritability ( $h^2$ ) using *mmer* function in *sommer* (Covarrubias-Pazarán 2016). Only  $h^2$  was calculated since the purpose was to compare trait  $h^2$  to simulated traits where we were limited to only additive effects. Standard error was estimated using the delta method (Holland et al. 2010) using the *pin* function in *sommer*.

We conducted a PC analysis (PCA) on BLUPs of 21 of the 23 traits using 259 lines (reduced from 281 due to missing data) using R function *prcomp*. Two traits, GDD to silk and GDD to tassel, were not included in the PCA because they were used as covariates in all GWAS models except for the univariate GWAS models with GDD to silk and GDD to tassel as the response variables. To ensure that none of these traits had an unwieldy influence on the resulting PCs, all 21 of these traits were centered and scaled prior to conducting the PCA. Three of the

resulting PCs had a  $h^2$  of zero and were not considered for PC GWAS (Supplementary Table S2). In total, 18 PC GWASs were conducted.

Two different marker sets were used in this study. Both sets were filtered to only include biallelic markers with minor allele frequency (MAF) 0.05. The first set, used for the analysis of the publicly available traits, consisted of 327,056 SNPs (B73 RefGen\_v4) from Bukowski et al. 2018. The second marker set, used for the simulation study, was the Illumina MaizeSNP50 BeadChip (Cook et al. 2012) and had 49,280 SNPs (B73 RefGen\_v3) available for analysis. Missing marker data were imputed with the software LinkImpute (Money et al. 2015), which implements an LD-based approach to infer nearest-neighbor information for imputation.

## Univariate and multivariate GWASs

The unified MLM (Yu et al. 2006) was used to conduct both univariate and multivariate GWASs. Briefly, the unified MLM is written as follows:

$$\mathbf{Y} = \mathbf{Q}\boldsymbol{\gamma} + \mathbf{G}\boldsymbol{\alpha} + \mathbf{Z}\mathbf{u} + \boldsymbol{\epsilon}, \quad (2)$$

where  $\mathbf{Y}$  is an  $n$ -by- $t$  matrix with  $n$  being the number of observations and  $t$  being the number of traits;  $\mathbf{Q}$  is the  $n$ -by- $(p+1)$  incidence matrix corresponding to the intercept and  $p$  fixed-effect covariates (i.e. PCs) accounting for subpopulation structure; all models, except the univariate analysis of GDD to silk and GDD to tassel, also included these two traits among the  $p$  fixed-effect covariates;  $\boldsymbol{\gamma}$  is a  $(p+1)$ -by- $t$  matrix of fixed effects of these covariates;  $\mathbf{G}$  is an  $n$ -by-1 vector of observed genotypes (coded  $-1, 0$  or  $1$ ) at the tested marker;  $\boldsymbol{\alpha}$  is a  $1$ -by- $t$  matrix of additive effects at the tested marker  $\mathbf{Y}$ ;  $\mathbf{Z}$  is an  $n$ -by- $n$  incidence matrix relating  $\mathbf{u}$  to  $\mathbf{Y}$ ;  $\mathbf{u} \sim \text{MVN}(\mathbf{0}, 2\mathbf{K}\sigma_g^2)$  is an  $n$ -by- $n$  matrix of genotype effects, where  $\mathbf{K}$  is an  $n$ -by- $n$  kinship matrix measuring the degree of familial relatedness between observations and  $\sigma_g^2$  is the genetic variance; and  $\boldsymbol{\epsilon} \sim \text{MVN}(\mathbf{0}, \mathbf{I}\sigma_e^2)$  is the  $n$ -by- $t$ -dimensional residual error with variance with  $\mathbf{I}$  being the identity matrix and  $\sigma_e^2$  being the residual variance. Note that  $\mathbf{Y}$ ,  $\boldsymbol{\gamma}$ ,  $\mathbf{u}$  and  $\boldsymbol{\epsilon}$  will collapse to a vector and  $\boldsymbol{\alpha}$  will collapse to a scalar, if only one trait is being analyzed. The MLM fitted to more than one trait is referred to as the mvMLM for the remainder of the article.

The MLM was fit univariately at each SNP with MAF 0.05, for the 23 trait BLUPs as well as 18 PCs. In addition, mvMLM was fit for three trait BLUPs (TPB, ULA and ERN). Traits TPB and ULA were of particular interest due to the extensive understanding of the pleiotropic nature of *Ig1* (Foster et al. 2004, Brown et al. 2011, Tian et al. 2011, Lewis et al. 2014, Wu et al. 2016) and



supporting evidence for further pleiotropy in expression data (Johnston et al. 2014). In addition, ear development, particularly ERN resulting from detriministic meristems, is well documented as being coordinated with tassel development (Vollbrecht et al. 2005, Bortiri et al. 2006, Satoh-Nagasawa et al. 2006). For both univariate MLM and mvMLM, a VanRaden additive genomic relationship matrix was used to estimate  $K$  (VanRaden 2008) and the first five PCs of the genomic markers were included in  $Q$  to account for population structure, with the optimal number selected being based on the Bayesian information criteria (BIC; Schwarz 1978). A LOCO approach that has been previously described (Rincet et al. 2014, Chen and Lipka 2016) was used for kinship estimation for the univariate models. In brief, LOCO procedure calculates a separate kinship matrix for each chromosome, where the kinship matrix for the  $i$ th chromosome does not use any markers from that chromosome in its calculations. Univariate MLM GWAS on the BLUPs and PC GWAS were conducted in R using GAPIT (Lipka et al. 2012), while mvMLM GWAS was conducted using the software GEMMA (Zhou and Stephens 2014). We used the Benjamini and Hochberg (1995) procedure to control for an FDR of 5% and 10%. The genetic correlations between traits were calculated as the Pearson correlation coefficient between marker effect sizes (van Rheenen et al. 2019), and this was contrasted to the pairwise Pearson correlation between trait BLUPs.

## Simulation study

To compare the true- and false-positive QTN detection rates for each of these GWAS approaches, we simulated six groups of three correlated phenotypes with contrasting genetic architectures using SNPs from the MaizeSNP50 BeadChip set (Cook et al. 2012). Simulated traits were created using the R package simplePHENOTYPES (Fernandes and Lipka 2020). The genetic architectures of these phenotypes differed by their QTN additive effect sizes, how many of the QTN were pleiotropic, and the narrow-sense heritability (see Table 2 for a summary of the considered genetic architectures). The additive effects of each set of pleiotropic and non-pleiotropic QTN followed a geometric series [described in Lande and Thompson (1990), Yu et al. (2008), Chen et al. (2019), Rice and Lipka (2019)]. Thus, the effect size of the  $i$ th QTN in a given set of QTNs was  $k^i$ , where  $k \in (0, 1)$ . For each setting, a total of three pleiotropic QTNs were simulated. Effect sizes were constant across settings; i.e. for each triplet of simulated correlated traits, the largest QTN effect size was 0.9, 0.5 and 0.1. The narrow-sense heritabilities that were considered were  $h^2 = 0.9, 0.5$  and  $0.2$  (Table 2). A total of 1,000 replicates of a ‘null’ setting where no QTNs were selected and heritability was zero were generated to rigorously test false-positive rates; the remaining settings were replicated 100 times. Each replicate had casual SNPs chosen at random with no bias toward selecting markers associated with population structure and therefore covariates (i.e. PCs of the markers) to control for population structure were not necessary to include for both univariate and multivariate GWASs. For each replicate of the simulation setting, all of the aforementioned GWAS approaches were performed.

To enable a thorough evaluation of the true- and false-positive QTN detection rates across a variety of conservative and anticonservative multiple testing adjustments, four different criteria were used to declare a marker–trait association to be statistically significant: (i) the Benjamini and Hochberg (1995) procedure to control the FDR at 5%, (ii) the Benjamini and Hochberg (1995) procedure to control the FDR at 10%, (iii) the Bonferroni procedure to control the genome-wide type I error rate at  $\alpha = 0.05$ , and (iv) the Bonferroni procedure to control the genome-wide type I error rate at  $\alpha = 0.10$ . For a given trait, a true positive was defined as the presence of at least one significantly associated SNP within  $\pm 250$  kb of a simulated QTN, while a false positive was defined the presence of at least one significantly associated SNP located outside of the  $\pm 250$  kb windows of all of the simulated QTNs. The  $\pm 250$ -kb window size was chosen based on the previous work done in the same diversity panel to describe regions of genomic proximity (Lipka et al. 2013).

## Data Availability

Supplementary materials are available online. All raw phenotypic and genotypic resources used are publicly available and can be accessed via [www.panzea.org](http://www.panzea.org). Trait BLUP data and

scripts used to analyze these BLUPs and conduct the simulation studies are freely available to the public at <https://github.com/lipka-lab/Multi-Trait-GWAS-Methods-Reveal-Loci-Associated-with-Maize-Inflorescence-and-Leaf-Architecture>.

## Supplementary Data

Supplementary data are available at PCP online.

## Acknowledgments

We would like to thank the two anonymous reviewers, as well as Dr. Marcus O. Olatoye, for their feedback and suggestions on making this manuscript stronger.

## Funding

National Science Foundation Plant Genome Research Project (1733606).

## Disclosure

The authors have no conflicts of interest to declare.

## References

- Aschard, H., Vilhjálmsson, B.J., Greliche, N., Morange, P.E., Tréguët, D.A. and Kraft, P. (2014) Maximizing the power of principal-component analysis of correlated phenotypes in genome-wide association studies. *Am. J. Hum. Genet.* 94: 662–676.
- Avery, C.L., He, Q., North, K.E., Ambite, J.L., Boerwinkle, E., Fornage, M., et al. (2011) A phenomics-based strategy identifies loci on APOC1, BRAP, and PLGG1 associated with metabolic syndrome phenotype domains. *PLoS Genet.* 7: e1002322.
- Bates, D., Mächler, M., Bolker, B.M. and Walker, S.C. (2015) Fitting linear mixed-effects models using lme4. *J. Stat. Soft.* 67: 1–48.
- Benjamini, Y. and Hochberg, Y. (1995) Controlling the false discovery rate: a practical and powerful approach to multiple testing. *J. R. Stat. Soc. B* 57: 289–300.
- Bonnett, O.T. (1954) The inflorescences of maize. *Science* 120: 77–87.
- Bortiri, E., Chuck, G., Vollbrecht, E., Rocheford, T., Martienssen, R. and Hake, S. (2006) JBL-660-2013 Wlaler Alvarado, Mauricio Bonilla (Horario de los estudiantes del CTP Hojanca). *Plant Cell* 18: 574–585.
- Bouchet, S., Servin, B., Bertin, P., Madur, D., Combes, V., Dumas, F., et al. (2013) Adaptation of maize to temperate climates: mid-density genome-wide association genetics and diversity patterns reveal key genomic regions, with a major contribution of the Vgt2 (ZCN8) locus. *PLoS One* 8: e71377.
- Brown, P.J., Upadaya, N., Mahone, G.S., Tian, F., Bradbury, P.J., Myles, S., et al. (2011) Distinct genetic architectures for male and female inflorescence traits of maize. *PLoS Genet.* 7: e1002383.
- Buckler, E.S., Holland, J.B., Bradbury, P.J., Acharya, C.B., Brown, P.J., Browne, C., et al. (2009) The genetic architecture of maize flowering time. *Science* 325: 714–718.
- Bukowski, R., Guo, X., Lu, Y., Zou, C., He, B., Rong, Z., et al. (2018) Construction of the third-generation *Zea mays* haplotype map. *GigaScience* 7: 1–12.
- Calderón, C.I., Yandell, B.S. and Doebley, J.F. (2016) Fine mapping of a QTL associated with kernel row number on chromosome 1 of maize. *PLoS One* 11: e0150276.

- Carlson, M.O., Montilla-Bascón, G., Hoekenga, O.A., Tinker, N.A., Poland, J., Baseggio, M., et al. (2019) Multivariate genome-wide association analyses reveal the genetic basis of seed fatty acid composition in oat (*Avena sativa* L.). *G3* 9: 2963–2975.
- Chai, L., Chen, Z., Bian, R., Zhai, H., Cheng, X., Peng, H., et al. (2018) Dissection of two quantitative trait loci with pleiotropic effects on plant height and spike length linked in coupling phase on the short arm of chromosome 2D of common wheat (*Triticum aestivum* L.). *Theor. Appl. Genet.* 131: 2621–2637.
- Chen, A.H., Ge, W., Metcalf, W., Jakobsson, E., Mainzer, L.S. and Lipka, A.E. (2019) An assessment of true and false positive detection rates of stepwise epistatic model selection as a function of sample size and number of markers. *Heredity* 122: 660–671.
- Chen, A.H. and Lipka, A.E. (2016) The use of targeted marker subsets to account for population structure and relatedness in genome-wide association studies of maize (*Zea mays* L.). *G3* 6: 2365–2374.
- Cook, J.P., McMullen, M.D., Holland, J.B., Tian, F., Bradbury, P., Ross-Ibarra, J., et al. (2012) Genetic architecture of maize kernel composition in the nested association mapping and inbred association panels. *Plant Physiol.* 158: 824–834.
- Covarrubias-Pazaran, G. (2016) Genome-assisted prediction of quantitative traits using the *r* package Sommer. *PLoS One* 11: e0156744–15.
- Fatumo, S., Carstensen, T., Nashiru, O., Gurdasani, D., Sandhu, M. and Kaleebu, P. (2019) Complimentary methods for multivariate genome-wide association study identify new susceptibility genes for blood cell traits. *Front. Genet.* 10: 1–13.
- Fernandes, S.B., Dias, K.O.G., Ferreira, D.F. and Brown, P.J. (2018) Efficiency of multi-trait, indirect, and trait-assisted genomic selection for improvement of biomass sorghum. *Theor. Appl. Genet.* 131: 747–755.
- Fernandes, S.B. and Lipka, A.E. (2020) simplePHENOTYPES: SIMulation of Pleiotropic, Linked and Epistatic PHENOTYPES. *BioRxiv*. doi: [10.1101/2020.01.11.902874](https://doi.org/10.1101/2020.01.11.902874).
- Flint-Garcia, S.A., Thuillet, A.C., Yu, J., Pressoir, G., Romero, S.M., Mitchell, S. E., et al. (2005) Maize association population: a high-resolution platform for quantitative trait locus dissection. *Plant J.* 44: 1054–1064.
- Foster, T., Hay, A., Johnston, R. and Hake, S. (2004) The establishment of axial patterning in the maize leaf. *Development* 131: 3921–3929.
- Frane, A.V. (2015) Are per-family type I error rates relevant in social and behavioral science? *J. Mod. Appl. Stat. Meth.* 14: 12–23.
- Galesloot, T.E., Van Steen, K., Kiemeneij, L.A.L.M., Janss, L.L. and Vermeulen, S.H. (2014) A comparison of multivariate genome-wide association methods. *PLoS One* 9: e95923.
- Gianola, D., Campos, G.D.L., Toro, M.A. and Naya, H. (2020) Do molecular markers inform about pleiotropy? 201: 23–29.
- Gilchrist, W.G. (2000). Statistical modelling with quantile functions. In *Statistical Modelling with Quantile Functions*. Chapman & Hall/CRC, Boca Raton.
- Holland, J.B., Nyquist, W.E. and Cervantes-Martínez, C.T. (2010) Estimating and interpreting heritability for plant breeding: an update. *Plant Breed. Rev.* 2003: 9–112.
- Hotelling, H. (1933) Analysis of a complex of statistical variables into principal components. *J. Educ. Psychol.* 24: 498–520.
- Huang, J., Johnson, A.D. and Donnell, C.J.O. (2011) PRIME: a method for characterization and evaluation of pleiotropic regions from multiple genome-wide association studies. *Bioinformatics* 27: 1201–1206. doi: [10.1093/bioinformatics/btr116](https://doi.org/10.1093/bioinformatics/btr116).
- Jia, Y. and Jannink, J.L. (2012) Multiple-trait genomic selection methods increase genetic value prediction accuracy. *Genetics* 192: 1513–1522.
- Johnston, R., Wang, M., Sun, Q., Sylvester, A.W., Hake, S. and Scanlon, M.J. (2014) Transcriptomic analyses indicate that maize ligule development recapitulates gene expression patterns that occur during lateral organ initiation open. *Plant Cell* 26: 4718–4732.
- Klei, L., Luca, D., Devlin, B. and Roeder, K. (2008) Pleiotropy and principal components of heritability combine to increase power for association analysis. *Genet. Epidemiol.* 32: 9–19.
- Lande, R. and Thompson, R. (1990) Efficiency of marker-assisted selection in the improvement of quantitative traits. *Genetics* 124: 743–756.
- Lewis, M.W., Bolduc, N., Hake, K., Htike, Y., Hay, A., Candela, H., et al. (2014) Gene regulatory interactions at lateral organ boundaries in maize. *Development* 141: 4590–4597.
- Li, C., Li, Y., Shi, Y., Song, Y., Zhang, D., Buckler, E.S., et al. (2015) Genetic control of the leaf angle and leaf orientation value as revealed by ultra-high density maps in three connected maize populations. *PLoS One* 10: 1–13.
- Lipka, A.E., Gore, M.A., Magallanes-Lundback, M., Mesberg, A., Lin, H., Tiede, T., et al. (2013) Genome-wide association study and pathway-level analysis of tocochromanol levels in maize grain. *G3* 3: 1287–1299.
- Lipka, A.E., Tian, F., Wang, Q., Peiffer, J., Li, M., Bradbury, P.J., et al. (2012) GAPIT: genome association and prediction integrated tool. *Bioinformatics* 28: 2397–2399.
- Liu, F., van der Lijn, F., Schurmann, C., Zhu, G., Chakravarty, M.M., Hysi, P.G., et al. (2012) A genome-wide association study identifies five loci influencing facial morphology in Europeans. *PLoS Genet.* 8: e1002932.
- McMullen, M.D., Bradbury, P., Flint-Garcia, S., Browne, C., Eller, M., Guill, K., et al. (2009) Genetic properties of the maize nested association mapping population. *Science* 325: 737–740.
- Money, D., Gardner, K., Migicovsky, Z., Schwaninger, H., Zhong, G.Y. and Myles, S. (2015) LinkImpute: Fast and accurate genotype imputation for nonmodel organisms. *G3* 5: 2383–2390.
- O'Reilly, P.F., Hoggart, C.J., Pomyen, Y., Calboli, F.C.F., Elliott, P., Jarvelin, M.R., et al. (2012) MultiPhen: joint model of multiple phenotypes can increase discovery in GWAS. *PLoS One* 7: e34861.
- Pan, Q., Xu, Y., Li, K., Peng, Y., Zhan, W., Li, W., et al. (2017) The genetic basis of plant architecture in 10 maize recombinant inbred line populations. *Plant Physiol.* 175: 858–873.
- Peiffer, J.A., Romay, M.C., Gore, M.A., Flint-Garcia, S.A., Zhang, Z., Millard, M. J., et al. (2014) The genetic architecture of maize height. *Genetics* 196: 1337–1356.
- R Core Team (2019) R: A Language and Environment for Statistical Computing. R Foundation for Statistical Computing, Vienna, Austria. <https://www.r-project.org/>.
- Rice, B. and Lipka, A.E. (2019). Evaluation of RR-BLUP genomic selection models that incorporate peak genome-wide association study signals in maize and sorghum. *The Plant Genome* 12: 1–14.
- Rincint, R., Moreau, L., Monod, H., Kuhn, E., Melchinger, A.E., Malvar, R.A., et al. (2014) Recovering power in association mapping panels with variable levels of linkage disequilibrium. *Genetics* 197: 375–387.
- Satoh-Nagasawa, N., Nagasawa, N., Malcomber, S., Sakai, H. and Jackson, D. (2006) A trehalose metabolic enzyme controls inflorescence architecture in maize. *Nature* 441: 227–230.
- Schwarz, G. (1978) Estimating the dimension of a model. *Ann. Stat.* 6: 461–464.
- Shi, D. y., Li, Y. h., Zhang, J. W., Liu, P., Zhao, B. and Dong, S. T. (2016) Increased plant density and reduced N rate lead to more grain yield and higher resource utilization in summer maize. *J. Integr. Agric.* 15: 2515–2528.
- Sluis, S., Van Der Posthuma, D. and Dolan, C.V. (2013) TATES: efficient multivariate genotype-phenotype analysis for genome-wide association studies. *PLoS Genet* 9: e1003235.
- Solovieff, N. (2013) Pleiotropy in complex traits: challenges and strategies. *Nat. Rev. Genet* 14: 483–495.
- Stearns, F.W. (2010) One hundred years of pleiotropy: a retrospective. *Genetics* 186: 767–773.
- Tian, F., Bradbury, P.J., Brown, P.J., Hung, H., Sun, Q., Flint-Garcia, S., et al. (2011) Genome-wide association study of leaf architecture in the maize nested association mapping population. *Nat Genet* 43: 6–11
- van den Boogaart, K.G. and Tolosana-Delgado, R. (2008) “compositions”: a unified R package to analyze compositional data. *Comput. Geosci.* 34: 320–338.
- van Rheenen, W., Peyrot, W.J., Schork, A.J., Lee, S.H. and Wray, N.R. (2019) Genetic correlations of polygenic disease traits: from theory to practice. *Nat. Rev. Genet.* 20: 567–581.
- Visscher, P.M. and Yang, J. (2016) A plethora of pleiotropy across complex traits. *Nat. Genet.* 48: 707–708.

- Vollbrecht, E., Springer, P.S., Goh, L., Buckler Iv, E.S. and Martienssen, R. (2005) Architecture of floral branch systems in maize and related grasses. *Nature* 436: 1119–1126.
- Wei, L.J. and Johnson, W.E. (1985) Combining dependent tests with incomplete repeated measurements. *Biometrika* 72: 359–364.
- Wu, X., Li, Y., Shi, Y., Song, Y., Zhang, D., Li, C., et al. (2016) Joint-linkage mapping and GWAS reveal extensive genetic loci that regulate male inflorescence size in maize. *Plant Biotechnol. J.* 14: 1551–1562.
- Yu, J., Holland, J.B., McMullen, M.D. and Buckler, E.S. (2008) Genetic design and statistical power of nested association mapping in maize. *Genetics* 551: 539–551.
- Yu, J., Pressoir, G., Briggs, W.H., Bi, I.V., Yamasaki, M., Doebley, J.F., et al. (2006) A unified mixed-model method for association mapping that accounts for multiple levels of relatedness. *Nat. Genet.* 38: 203–208.
- Zhang, W., Gao, X., Shi, X., Zhu, B., Wang, Z., Gao, H., et al. (2018) PCA-based multiple-trait GWAS analysis: a powerful model for exploring pleiotropy. *Animals* 8: 239.
- Zhou, X. and Stephens, M. (2014) Efficient multivariate linear mixed model algorithms for genome-wide association studies. *Nat Met* 11: 407–409.